Supporting Information

Chen et al. 10.1073/pnas.0810992106

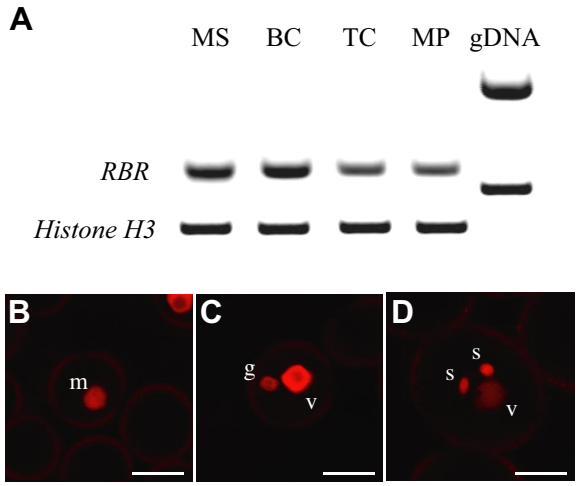

Fig. S1. Expression of *RBR* in pollen. (*A*) RT-PCR analysis of *RBR* expression with RNA extracted from isolated spores at 4 stages of pollen development. High levels of transcript levels are present at the microspore stage (*MS*) and in bi-cellular pollen (*BC*), followed by small decline in tri-cellular (*TC*) and mature pollen (*MP*). Histone variant *H3.2* (At4g40040) was used as a control. (*B-D*) We studied the expression pattern of RBR at the cellular level using the expression of the translational reporter construct p*RBR-RBR::RFP*, which complements partially *rbr-2* (Table S1 and Fig. S2*B*). We observed the expression of RBR-RFP in microspore (*B*), and developing pollen at bi-cellular stage (*C*) and tri-cellular stage (*D*). (Scale bars, 10 μm.) *m*, microspore nucleus; *v*, vegetative cell nucleus; *g*, generative cell nucleus; *s*, sperm cell nucleus.

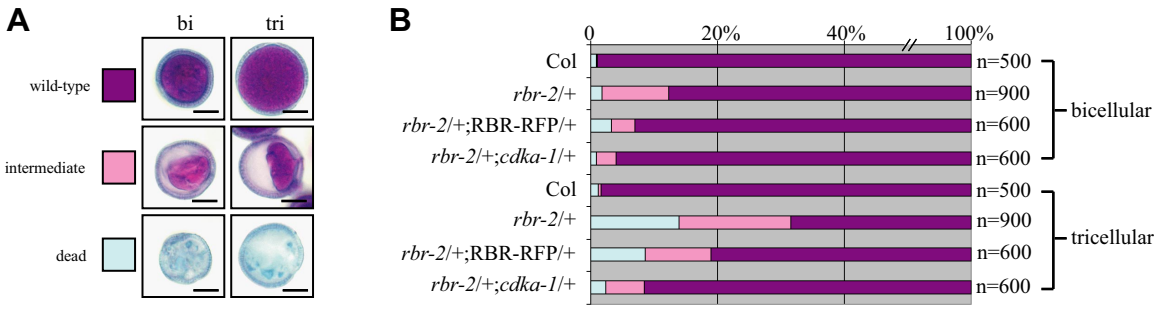

Fig. S2. Pollen death in *rbr* mutants. (*A*) Alexander staining viability analysis showing WT pollen (purple), intermediate pollen (pink), and dead pollen (green) at bi-cellular and tri-cellular stages, respectively. (Scale bars, 10 μm.) (*B*) Bar chart showing percentage of 3 types of pollen from Col, *rbr-2*/+, *rbr-2*/+;RBR-RFP/+, and *rbr-2*/+;*cdka-1*/+, at bi-cellular and tri-cellular stages, respectively. The size of total population analyzed (*n*) is indicated (*Right*).

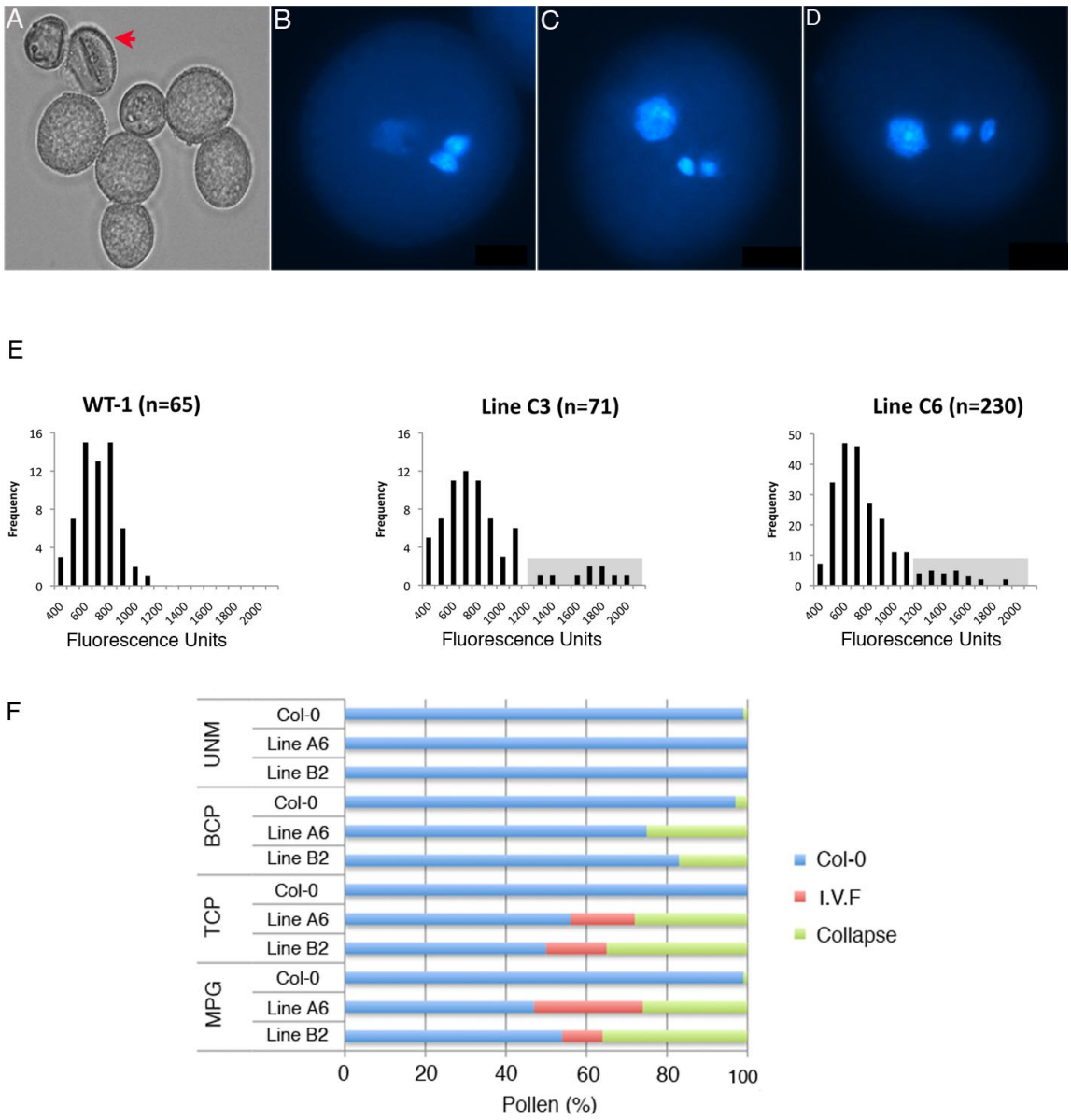

Fig. S3. Induced effect of *LAT52*-hp*RBR* construct during pollen development. Cytological analysis of plants expressing hairpin dsRNA targeted to *RBR* mRNA specifically in the vegetative cell. (*A*) DIC image showing aborted pollen grains (red arrow) at the mature pollen stage. (*B-D*) DAPI stained mature pollen grains with a WT phenotype (*B*) and those with a novel phenotype showing increased vegetative nuclear intravascular fluorescent (*I.V.F.*) from 2 independent siblings (*C* and *D*). (*E*) Measurement of vegetative cell nucleus fluorescence following DAPI staining at the mature pollen stage emphasizing the new class of pollen grains (shaded box) with fluorescence units above that observed in the WT populations. Number of pollen grains analyzed are indicated in the parenthesis. Fluorescence intensity was measured using a Nikon TE2000 fluorescence microscope and OpenLab 5.0.2 software (Improvision). (*F*) Phenotypic analysis of 2 independent siblings at the uni-cellular microspore (*UNM*), bi-cellular pollen (*BCP*), tri-cellular pollen (*TCP*), and at mature pollen stage (*MPG*). Bar chart showing the origin of the aborted and I.V.F. phenotype as observed in 2 independent siblings. The aborted phenotype was traced to the bi-cellular stage, whereas the I.V.F. phenotype was initially detected at the tri-cellular stage and increased in mature pollen for line A6 but decreased in line B2.

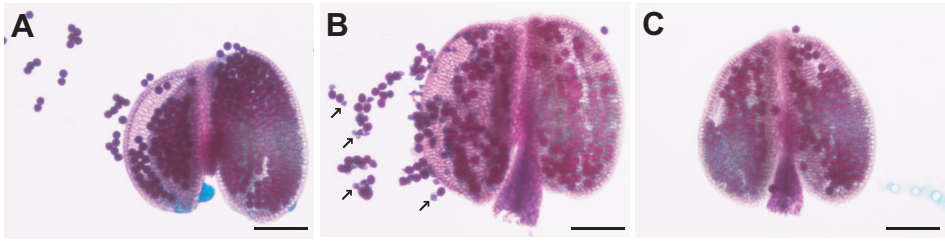

Fig. S4. Pollen death in *rbr* mutants and the rescue of pollen death by *cdka-1*. Alexander staining of Col (*A*), *rbr-2*/+ (*B*), and *rbr-2*/+;*cdka-1*/+ (*C*) anthers. Arrows indicate dead pollen. (Scale bars, 100 μm.)

Table S1. Paternal transmission of *rbr-2* and *cdka-1* alleles

Female × Male	Mean transmission ± SD (mutant allele) in F1, %	Transmission efficiency, %	n
Col × *rbr-2*/+	8.0 ± 2.8 (*rbr-2*)	8.7	637
Col × *rbr-2*/+;RBR-RFP+/−	20.2 ± 5.1(*rbr-2*)	25.3	816
Col × *cdka-1*/+	8.2 ± 2.1(*cdka-1*)	8.9	477
Col × *rbr-2*/+;*cdka-1*/+	47.0 ± 3.8 (*rbr-2*)	88.7	430

[a]Transmission efficiency is the number of mutant progeny divided by the number of WT progeny.